Responses to the comments of Referee #2

Article ID: essd-2024-2
Title: CIrrMap250: Annual maps of China's irrigated cropland from 2000 to 2020 developed through multisource data integration
Authors: Ling Zhang, Yanhua Xie, Xiufang Zhu, Qimin Ma, Luca Brocca

Dear Reviewer,

Thank you very much for the great efforts on our manuscript. Inspired by your valuable comments, we have made a major revision. The key revisions include:

(1) Analyzing and discussing uncertainties and potential applications of the CIrrMap250 product;
(2) Providing spatial trends in irrigated area from 2000 to 2020 at the subregional scale;
(3) Summarizing the descriptions, formulas, and sources of the different products and variables used in the study;
(4) Thoroughly revising the content and figures to improve readability, conciseness, and clarity.

The detailed point-to-point responses are as follows. Texts in red are the reviewer's comments; **those in black** are our responses to the reviewer's comments; and *those in blue and italics* are the revised texts appeared in the revised manuscript.

General summary:

This study presents the development of a multi-year (2000-2021) irrigated cropland map for China, named CIrrMap250. The authors employ a semi-automatic training approach integrating remote sensing data (vegetation indices, hybrid cropland products, and paddy field maps), county-level irrigation statistics and surveys, and an irrigation suitability map. Utilizing a threshold-calibration method and the random forest algorithm, the CIrrMap250 map is evaluated against reference sites and other large-scale irrigation maps, demonstrating superior accuracy. The study reveals a consistent net expansion of irrigated croplands in Northeast and Northwest China, with over 60% deemed unsustainable due to severe water stress. The CIrrMap250 map holds significant application potential for water resource management and food security. I have some comments below and please address them before this article can be published.

Thanks for the positive comments.

Major comments:

1 L74-81: China's vast agricultural landscape comprises diverse cropping systems and associated irrigation methods, such as rice paddies in the South and Northeast, and corn/wheat rotations in the North China Plain and Northwest. The study does not adequately address this diversity. It would be beneficial for the CIrrMap250 to provide detailed mappings for irrigation methods for associated crop types, if possible. Moreover, the integration of county-level yearbook data on irrigated crop types and rotations could enhance the map's specificity and utility. Clarifying how different cropping systems and crop types are distinguished would significantly improve the comprehensiveness of the methodology. For example, L123 - Mapping 30-m CCropLand30 cropland layer (available every 5-year) - does this dataset also tell you which crop type is associated with each pixel?

Response: Thank you for the insightful comments. It would indeed be ideal for irrigation mapping to include the full thematic detail required for agricultural monitoring, such as irrigation methods and crop types. However, there are two major challenges in achieving this.

First, to our knowledge, existing cropland data in China, including CCropLand30, only provide the spatial distribution of cropland without crop type information due to the diversity and complexity of agricultural systems (Zhang et al., 2022a; Van Tricht et al., 2023). While numerous studies have mapped some crops (e.g., wheat, rice and maize) across China, none of them have included all crop types and accounted for

mixed or sequential cropping practices (Dong et al., 2020; You et al., 2021; Shen et al., 2022; Mei et al., 2023; Shen et al., 2023; Zhang et al., 2024a). The mixed and sequential cropping practices are crucial because when a specific crop is mapped in a grid for a given month, the remaining crop types must be allocated to the rest of the available cropland area within that grid. This lack of cropland products that distinguish crop types limits the classification of irrigated versus rainfed crop types.

Second, although statistical yearbooks provide planted area for different crop types, they do not offer information on the irrigated versus rainfed area for each crop types, nor do they detail crop rotations. This also hinders the identification of irrigated versus non-irrigated crop types. Addressing these challenges and mapping the distribution of irrigated and rainfed crops is beyond the scope of this research but will be considered in our future work.

Regarding irrigation methods, there are indeed some statistical data on the areas of different irrigation methods (i.e., flood, drip, and sprinkler irrigation). However, spatially explicit allocation of irrigated areas by different methods is a significant challenge because irrigation methods cannot be easily distinguished by remote sensing data, except for certain systems like center pivot irrigation. This limitation is especially pronounced with coarse-resolution imagery such as MODIS.

2 Although the CIrrMap250 is purportedly an annual dataset, the primary analyses are based on three specific years (2000, 2010, and 2020). Although Figure 9 presents a 20-year timeseries of irrigated croplands in different regions, it is crucial to present the interannual variability of irrigation areas. Analyzing annual data across the entire 20-year period can reveal the influence of climatic factors, such as temperature and precipitation, on irrigation trends. Additionally, showcasing irrigation transitions in various regions, beyond the highlighted area between CSC and NC, would provide a more comprehensive view of national trends.

Response: The spatiotemporal changes in irrigated areas were analyzed based on the annual data of CIrrMap250, rather than three specific years (2000, 2010, and 2020), as shown in Figure 8 in the manuscript. Figure 8 shows the interannual trend of irrigated areas from 2000 to 2020 at the pixel scale (see below). Pixels with significant temporal changes (increasing or decreasing trend) in irrigated area ($p<0.05$) are marked as "expansion" or "reduction," while those with insignificant changes are marked as "stable." The inset panel at the top of the figure depicts the center-of-gravity movement (i.e., spatial trend) of China's irrigated areas at the national scale. Each circle in the inset panel corresponds to the gravity center of China's irrigated area for a specific year (ranging from 2000 to 2020).

We further analyzed the spatial trends in irrigated areas from 2000 to 2020 in each subregion of China. As shown in Supplementary Figure S5 (see below), the gravity center of irrigated areas showed clear trends in NWC, NEC, and NC but was insignificant in the remaining subregions. In NWC, the irrigated area significantly shifted to the northwest, while in NEC, it significantly shifted to the northeast. Meanwhile, there was a northward spatial trend in irrigated areas in NC.

The related results have been added in the revised manuscript

The gravity center showed clear trends in NWC, NEC, and NC but was insignificant in the remaining subregions (Supplementary Figure S5). In NWC, irrigation significantly shifted to the northwest, while in NEC, it significantly shifted to the northeast. Meanwhile, there was a northward spatial trend in irrigation in NC.

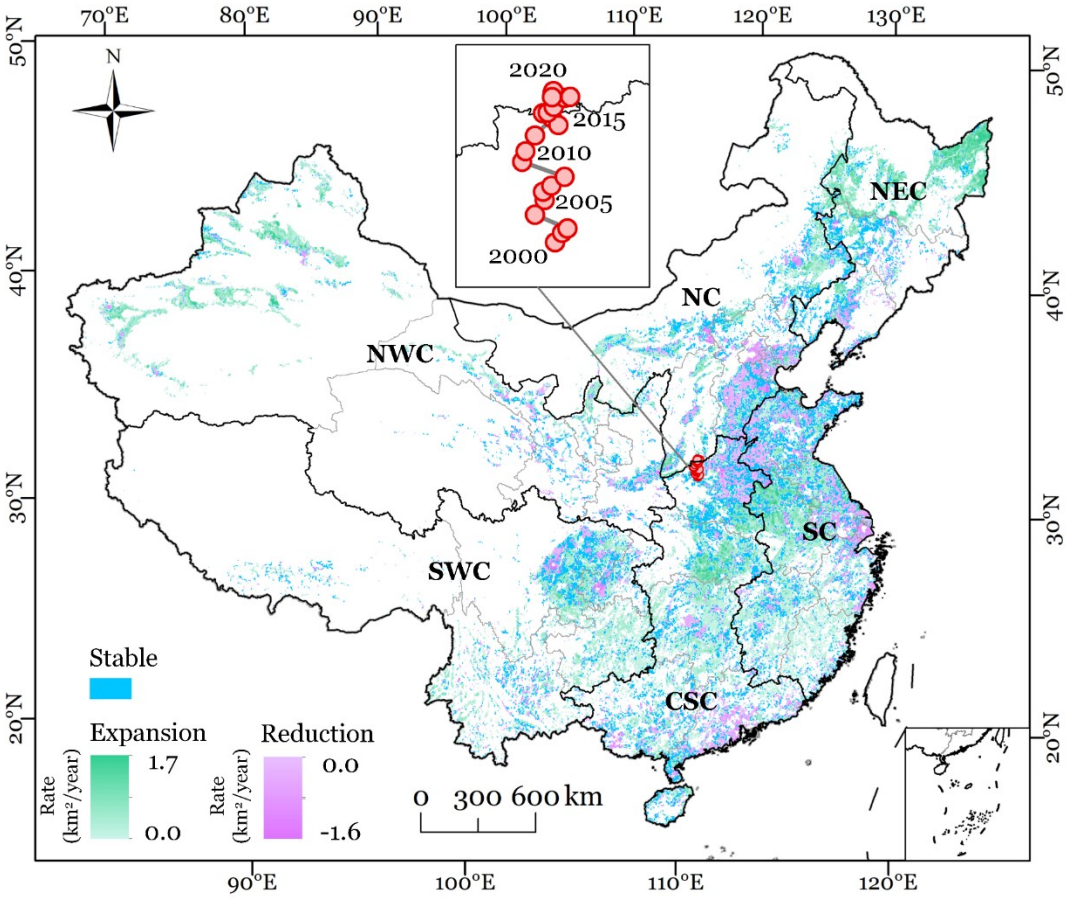

Figure 8. Spatiotemporal changes in irrigated area from 2000 to 2020. *Pixels exhibiting significant interannual trends ($p < 0.05$) in irrigated area were labelled as "expansion" or "reduction", while those with insignificant changes are denoted as "stable". Pixels with less than 5% irrigated croplands were excluded from the map. The inset panel on the top of the figure depicts the center-of-gravity movement (spatial trend) of China's irrigated areas at the national scale.*

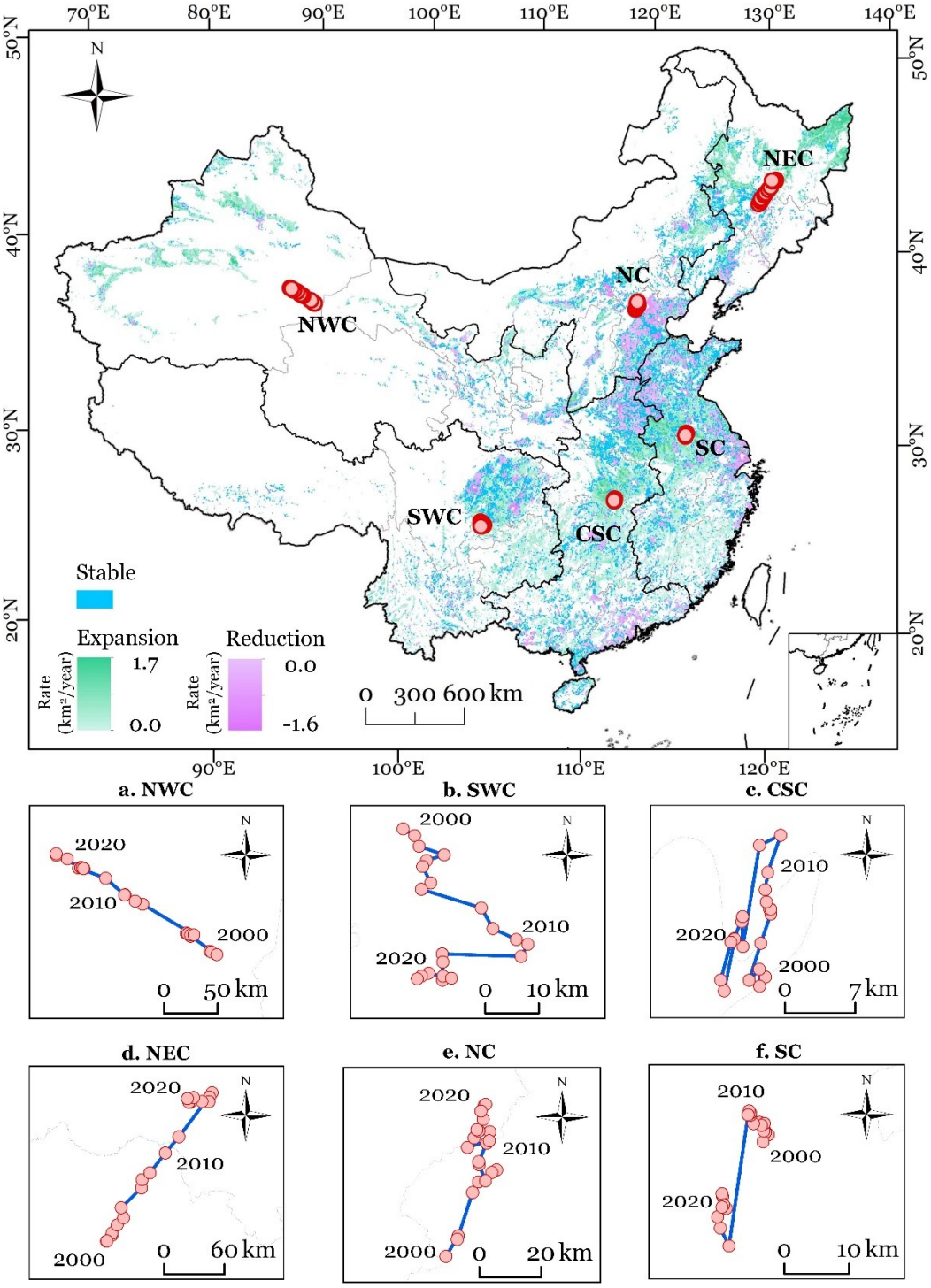

Figure S5. Spatial trends in irrigated areas from 2000 to 2020 in the six subregions of China. *The top panel shows the interannual trend in irrigated area at the pixel scale (same as Figure 8 in the main text) and illustrates the locations of the gravity centers of irrigated areas for each subregion. Panels a-d depict the center-of-gravity movement of irrigated areas from 2000 to 2020 in each subregion.*

3. Since this data product is a fusion of data from multiple sources, would it be good and necessary to quantify uncertainties of different sources? Such as the assumption outlined in 2.2.1, L151-155, and also in 2.2.2 L164-184. Section 5.2 L486-502 discussed the uncertainties and limitations. What are the limitations associated with integrating multiple sources? For example, for the same region, how do remote-sensing indices, statistics, and survey data differ from each other (or not)? In which regions does each index perform better? Please give some discussion as it may be useful to evaluate the CIrrMap250 product and provide future user information.

Response: Thanks for the comment. We agree that it is crucial to convey the underlying uncertainties of data from different sources and the final product. However, it is challenging for us to quantify uncertainties of each data source given the unavailability of ground reference data. Instead, we evaluated our final product CIrrMap250 and discussed possible product uncertainties in relation to data sources. To do so, we have conducted additional analyses and discussions on the uncertainties associated with CIrrMap250 (see below).

Despite the advancements of CIrrMap250 compared to existing products, we acknowledge several uncertainties and limitations associated with the product. CIrrMap250 was developed by integrating data from multiple sources using a semi-automatic training method, leveraging joint information related to irrigation in each data source. However, each data source inherently presents uncertainties and deficiencies (Shahriar Pervez et al., 2014; Tian et al., 2024). Irrigation area statistics, in particular, can contain significant uncertainties due to technical and political factors, such as variations in statistical method and administrative division (Thenkabail et al., 2009; Meier et al., 2018), which have not been well characterized. These biases and uncertainties would manifest in CIrrMap250, since our training samples were derived from these statistics-constrained irrigation maps. In this study, we addressed this issue by merging reported irrigation statistics with independent survey results. Nonetheless, uncertainties related to irrigated areas may remain unresolved in certain regions. For instance, we found considerable discrepancies between the statistical and surveyed irrigation areas in SC and NEC (Supplementary Figure S10a), implying greater uncertainties in these subregions compared to others. Furthermore, the irrigation statistics and surveys were reconciled with remote sensing data to address inconsistencies between the two sources. However, the bias ratio may be inaccurately estimated in the reconciliation process, introducing additional uncertainties to the results.

Cropland mask layers used to distinguish cropland from non-cropland are another source of uncertainty. These layers were constructed using our hybrid cropland product

(Zhang et al., 2024), which integrates five state-of-the-art remote sensing land use/cover products. This hybrid product significantly reduced uncertainties associated with cropland distribution in China. However, remote sensing-derived cropland data show large uncertainties in southern China. As illustrated in Supplementary Figure S10b, only 27% of croplands on average in SWC, SC, and CSC are consistently identified by remote sensing products, compared to 39% in northern subregions (NEC, NC, and NWC). These uncertainties are reflected in our hybrid cropland product, which shows greater accuracy in the northern subregions than in the southern ones (Supplementary Figure S10c). Meanwhile, the temporal resolution of the cropland layers is five years, which may not accurately capture changes in cropland distribution in regions experiencing rapid changes. The uncertainties and errors in the cropland mask layer, particularly in southern China, could propagate into CIrrMap250.

An additional source of uncertainty is the MODIS-derived vegetation indices (i.e., NDVI, EVI, and GI). These indices are prone to data gaps due to cloud and cloud shadow contaminations. In this study, we filled the data gaps by using a simple nearest neighbor interpolation method, which may introduce uncertainties to CIrrMap250. Additionally, irrigated croplands in humid southern China are more sparsely distributed and show weaker contrast with rainfed fields compared to northern China. This makes the peak vegetation indices less effective and more uncertain in distinguishing irrigated from rainfed cropland (Xie et al., 2019; Zhang et al., 2022a). Consequently, our CIrrMap250 product exhibits higher accuracy in NEC, NWC, and NC than in SC, CSC, and SWC subregions (Supplementary Figure S10d).

Lastly, CIrrMap250 has the limitation of a relatively coarse spatial resolution of 250 m and does not fully address the mixed-pixel problem. While CIrrMap250 offers a higher spatial resolution than many existing large-scale irrigation maps, it may not be suitable for local applications, such as field or irrigation district levels. The mixed-pixel problem significantly affects the precision of cropland masks (Zhang et al., 2024) and weakens the distinction between vegetation indices for irrigated and rainfed cropland. Even though CIrrMap250 considers the fractional coverage of cropland, it does not differentiate between irrigated and rainfed croplands at subpixel scales, like many other existing irrigation maps. There are many small and fragmented croplands in the mountainous regions of southern China. CIrrMap250 should be used with caution in these areas due to the prevalence of mixed pixels.

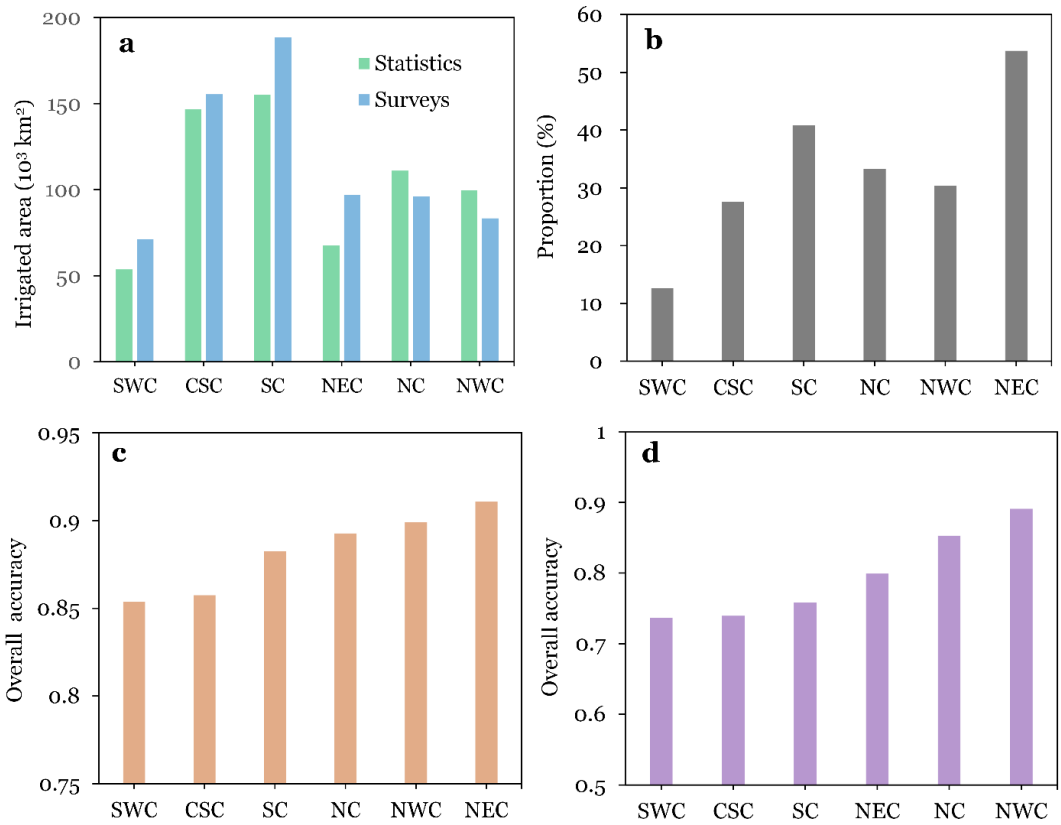

Figure S10. Uncertainty analysis of the CIrrMap250 product. ***a****. Comparison of statistics and surveys of irrigated area across different subregions.* ***b****. Proportion of croplands consistently identified by five state-of-the-art remote sensing land use/cover products, including GlobeLand30 (Chen et al., 2015), GLAD (Potapov et al., 2021), CLUD (Liu et al., 2014), CLCD (Yang and Huang, 2021), and CACD (Yu et al., 2021).* ***c****. Comparison of the accuracy of the hybrid cropland product CCropLand30 across different subregions.* ***d****. Comparison of the accuracy of CIrrMap250 (for the year 2010) across different subregions.*

4. The study employs numerous data products and indices, yet lacks clear definitions and descriptions. A detailed table in the main text or supplementary material, listing all data products used and indices defined, could enhance clarity. Including equations for calculating indices such as PET, aridity index, Water Scarcity Index (WSI), NDVI, EVI, and GI is essential for transparency. Defining WSI and its components, including whether groundwater pumping in North China is considered, would further elucidate the methodology. Providing detailed and comprehensive information, similar to the content in Tables S1-S3, would greatly benefit readers.

Response: Thank you for the suggestion. We have compiled a comprehensive list of

the products and variables utilized in this study, which can be found in Supplementary Table S2. Each entry in the table includes a detailed description, formula, and the respective data source. Please refer to the table below for details.

Table S2. Summary of the products and variables used in this study

Product /variable	*Description*	*Formula*	*Source*
CCropLand30	*Hybrid cropland product for China*	-	*Zhang et al. (2024)*
CLUD	*China's Land-use/cover dataset*	-	*Liu et al. (2014)*
NDVI/EVI/GI	*Normalized Vegetation Index / Enhanced Vegetation Index / Greenness Index*	*See Table S1*	*MODIS*[a]
Irrigation suitability	*Suitability of cropland for irrigation*	*Equation 4 in the main text*	*This study*[b]
SVI	*Irrigation suitability-adjusted peak vegetation index*	*Equation 5 in the main text*	*This study*[b]
Precipitation	*Annual precipitation*	$\sum_{i=1}^{Ydays} PCP_i$	*NMIC*[c]
Temperature	*Mean annual temperature*	$\frac{1}{Ydays}\sum_{i=1}^{Ydays} TMP_i$	*NMIC*[c]
PET	*Annual evapotranspiration*	$\sum_{i=1}^{Ydays} PET_i$	*This study*[b]
Aridity index	*Degree of dryness of the climate*	MA_PCP/MA_PET	*This study*[b]
Irrigation water withdrawal	*Total amount of water withdrawals used for crop irrigation*	-	*PWRD*[d]
WSI	*Water scarcity index*	TWU/WA	*Zhang et al. (2023)*
Cropping intensity	*Number of crops grown on the same field in a given agricultural year*	-	*Xu et al. (2017)*
Soil type	*Genetic soil classification system in China*	-	*RESDC*[e]
Elevation	*Mean elevation*	-	*SRTM*[f]

Slope	*Mean slope*	*-*	*This study[b]*
Distances to water bodies	*Euclidean distance to rivers, lakes, reservoirs, canals, and ponds*		*This study[b]*

Note. [a]indicates variables derived from Moderate Resolution Imaging Spectroradiometer (MODIS) data (https://modis.gsfc.nasa.gov/). [b]indicates variables generated in this study. [c]indicates the National Meteorological Information Center (http://data.cma.cn/). [d]indicates the provincial water resources departments. [e]indicates the Resource and Environment Science and Data Center (https://www.resdc.cn/Default.aspx). [f]indicates the Shuttle Radar Topography Mission (https://www.earthdata.nasa.gov/sensors/srtm). Ydays represents the number of days in a given year; PCP_i denotes the amount of precipitation at the ith day; TMP_i indicates mean air temperature at the ith day; PET_i represents evapotranspiration estimated using the Priestley-Taylor method (Priestley and Taylor, 1972); MA_PCP and MA_PET denote mean annual precipitation and PET, respectively; TWU represents total water use, including both groundwater and surface water withdrawals for irrigation, industry, domestic purposes, forestry, livestock, and fishery; WA represents water availability and refers to the total surface water and groundwater generated by precipitation.

5. 3.1 L219 - Can you also give a brief description of the threshold-calibration method, instead of stating "following the previous studies" - letting the readers of this paper understand your method is important. Particularly Equation 5 - how do you determine the threshold? Since you have 20-year data, is this threshold constant? Or does it change year-by-year? Please elaborate.

Response: We have provided a brief description of the threshold-calibration method, following your suggestion.

We applied a threshold-calibration method to automatically generate the training pool, following previous studies by Xie et al. (2019; 2021) and Zhang et al. (2022d). With this method, cropland pixels with annual peak vegetation greenness exceeding an optimized threshold were classified as "irrigated". The threshold was individually calibrated for each county and year using available irrigation statistics and surveys. Based on the calculated optimized thresholds, intermediate irrigation maps were generated at the county level. Pixels consistently classified as "irrigated" in all intermediate maps were identified as irrigation candidates, while those classified as "non-irrigated" were considered potential non-irrigated samples.

6. L223-226, please elaborate on this statement - "Cropland with lower elevation, gentler slope, and higher aridity index was hypothesized to have higher irrigation

suitability and potential" - is this statement a hypothesis? Or has it already been demonstrated in Liu et al.? It is not clear by now.

Response: Liu et al. (2022) did not directly validate this hypothesis but highlighted the significant role of geographical factors such as elevation, slope, and precipitation in shaping the spatial distribution of irrigated cropland in China using a Select K Best algorithm. Hence, it is a hypothesis that lower elevation, gentler slopes, and higher aridity indices characterize cropland areas with greater irrigation suitability and potential. This hypothesis aligns with previous studies (Worqlul et al., 2015; Worqlul et al., 2017; Li and Chen, 2020; Zhang et al., 2022b), and is proposed for following reasons.

In regions with higher elevations, accessing water resources becomes more challenging, reducing the likelihood of irrigation. For instance, our field observations on the Loess Plateau's high-elevation areas revealed that residents rely solely on deep wells for domestic water, with crop growth entirely dependent on rainfall. Moreover, agricultural productivity at higher altitudes in China is hindered by the absence of irrigation infrastructure and increased costs associated with transportation and labor. Meanwhile, areas with steeper slopes generally have lower water holding capacities and are less suitable for irrigation systems. Typically, slopes exceeding 8% are considered impractical for surface irrigation systems. Therefore, areas with gentler slopes are more conducive to the presence of irrigated cropland. Lastly, croplands with higher aridity indices, characterized by lower precipitation but higher potential evapotranspiration (PET), are also more likely to require irrigation due to greater water demand.

We have clarified the hypothesis in the new manuscript

A static irrigation suitability map was created based on elevation, slope, and aridity index of cropland. These factors play a crucial role in shaping the spatial distribution of irrigated cropland in China, as demonstrated by Liu et al. (2022). Cropland areas characterized by lower elevation, gentler slopes, and higher aridity indices were hypothesized to exhibit greater irrigation suitability and potential, in line with previous studies (Worqlul et al., 2015; Worqlul et al., 2017; Li and Chen, 2020; Zhang et al., 2022d).

7. L275-280 the description of Figure 2c and the figure caption don't match - Figure 2c shows 2010, but the text indicates 2020. Please check your text and figure captions. Also, since you can identify the center pivot irrigation system, can you also provide an irrigation method map, distinguishing between sprinkler irrigation (mostly in North China) and flood irrigation (more common in South China)?

Response: As shown in Figure 2 (see below), panel c shows the spatial distribution of the third-party samples in 2020. We have double-checked all the texts and figure captions carefully to ensure consistency.

Center pivot irrigation systems are identifiable in remote sensing imagery due to their distinctive circular irrigation pattern centered on pivots, which creates a unique visual signature on crops (Chen et al., 2023). However, other irrigation methods such as flood irrigation, drip irrigation, and sprinkler irrigation are not easily distinguishable using remote sensing data, especially using coarse-resolution datasets like MODIS.

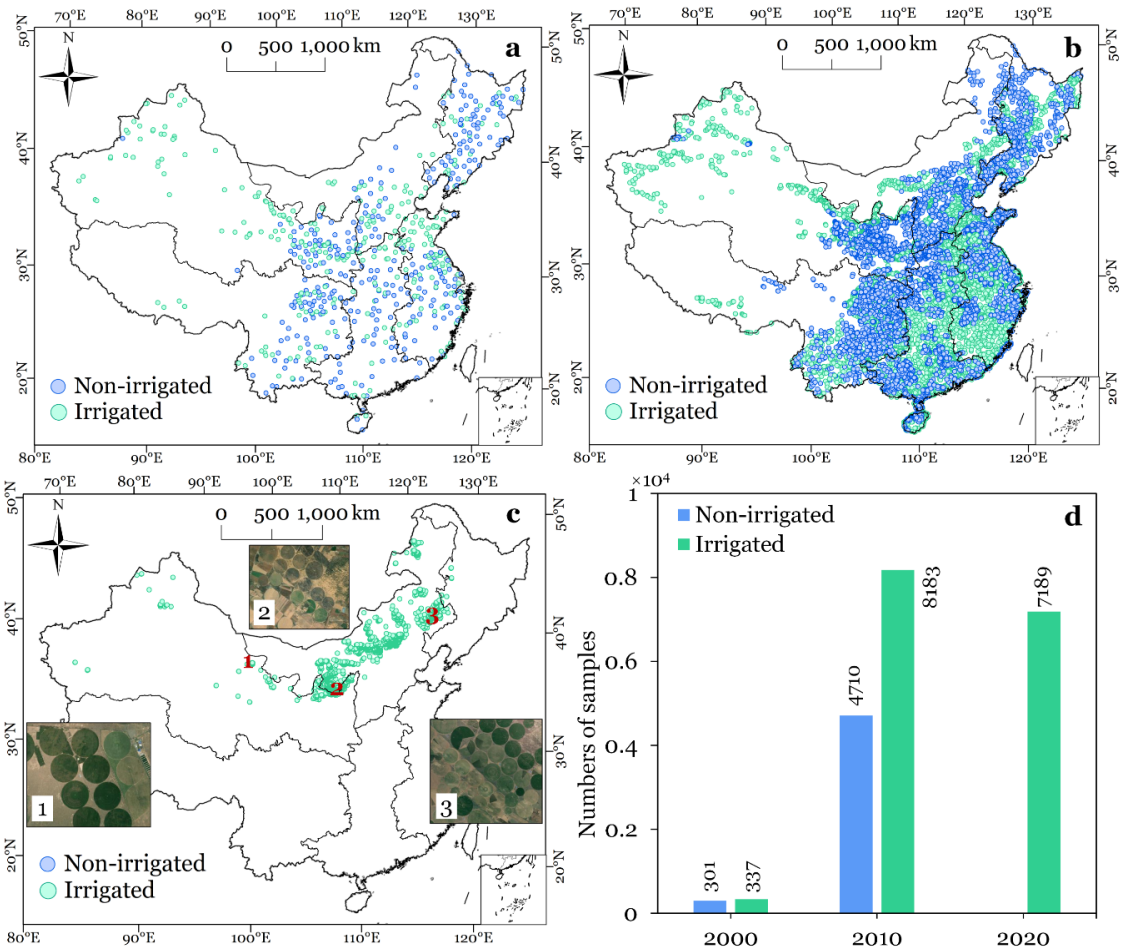

Figure 2. Spatial distribution of validation samples. ***a****, Spatial distribution of the third-party samples in 2000.* ***b****, Spatial distribution of the samples in 2010 retrieved from provincial land-use maps of China's second National Land Survey.* ***c****, Spatial distribution of the third-party samples in 2020.* ***d****, Numbers of irrigated and non-irrigated samples for different years.*

8. L337-340, please define WSI. What are the major water resources used in WSI? How about considering pumping groundwater for irrigation in North China? Is it a part of the WSI calculation and evaluation of the irrigation map?

Response: The Water Scarcity Index (WSI) is defined as the ratio of total water use (TWU) to water availability (WA), i.e., WSI = TWU/WA. This index quantifies the fraction of available water resources appropriated by humans. TWU encompasses both groundwater and surface water withdrawals for irrigation, industry, domestic purposes, forestry, livestock, and fishery. WA refers to the total surface water and groundwater generated by precipitation. The definition of WSI is provided in the main text of the new manuscript as well as in Table S2 of the Supplementary file.

The prefecture-level data on water scarcity index (WSI) for 2010-2020 were extracted from our previous study (Zhang et al., 2023b). WSI is defined as the ratio of total water use to water availability, as shown in Supplementary Table S2. Total water use encompasses both groundwater and surface water withdrawals for irrigation, industry, domestic purposes, forestry, livestock, and fishery. Water availability refers to the total surface water and groundwater generated by precipitation.

9. Figure 5, please give a scale legend for region A, B, C, and D. i.e., how big are these four regions?

Response: Thank you for your suggestion. In the revised figure, scale bars have been added for regions A, B, C, and D, as shown below.

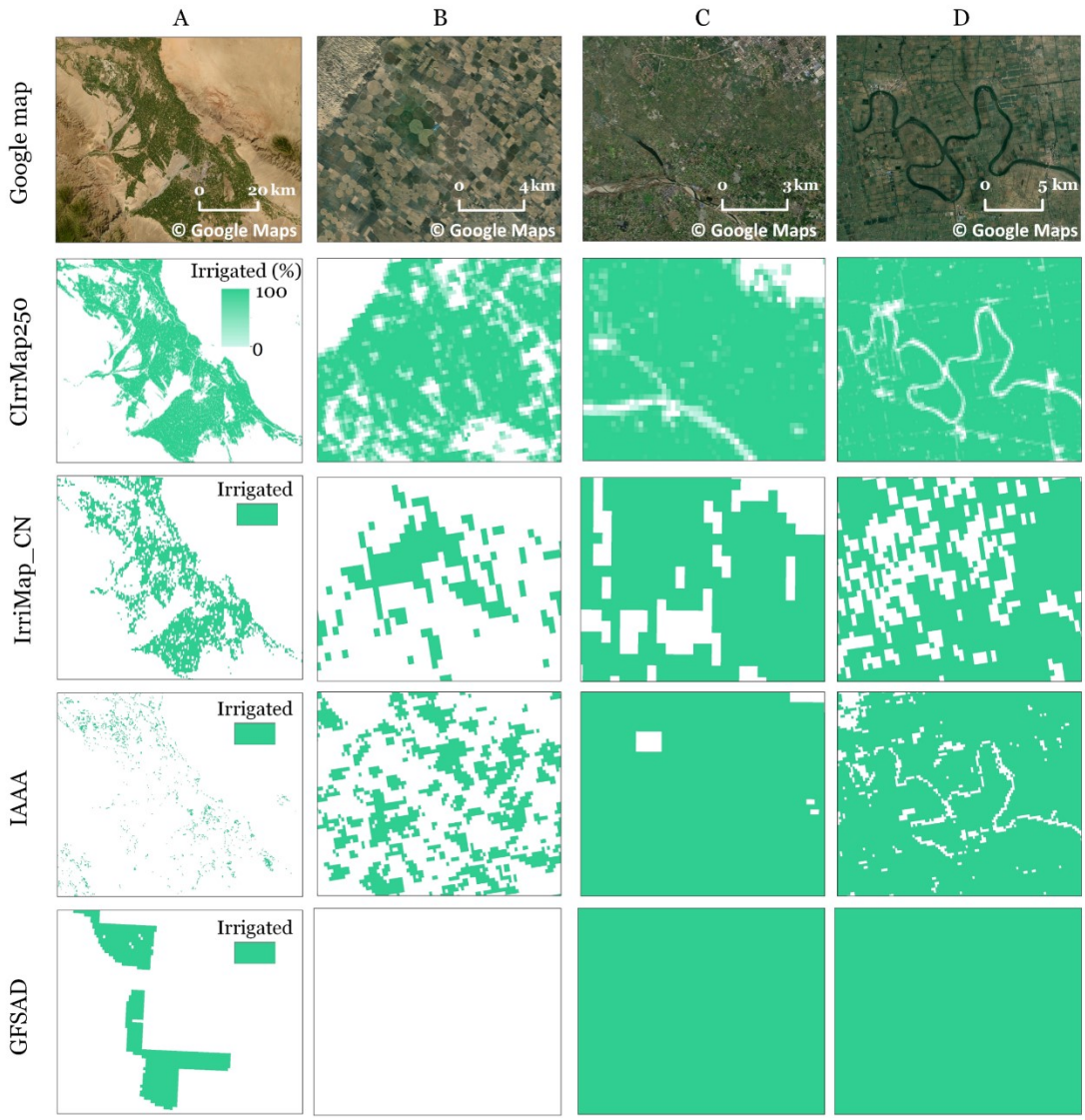

Figure 5. Visual comparison of CIrrMap250 with existing maps. *The five rows from top to bottom correspond to the Google map, CIrrMap250, IrriMap_CN, IAAA and GFSAD, respectively. Locations of the four selected zones are presented in Figure 4a.*

10. Figure 8. The transition only shows three years, 2000, 2010, and 2020. What about the interannual variability, since you have 20-year annual data? It would be good to show an interannual timeseries of irrigation transitions across China. Figure 8 highlights an area between CSC and NC; how about other regions in China? What are the transitions across regions over the 20-year period?

Response: The spatiotemporal changes in irrigated areas were analyzed based on the annual data of CIrrMap250, rather than three specific years (2000, 2010, and 2020). Figure 8 shows the interannual trend of irrigated areas from 2000 to 2020 at the pixel scale. Pixels with significant temporal changes (increasing or decreasing trend) in

irrigated area ($p<0.05$) are marked as "expansion" or "reduction," while those with insignificant changes are marked as "stable." The inset panel at the top of Figure 8 depicts the center-of-gravity movement (i.e., spatial trend) of China's irrigated areas at the national scale. Each circle in the inset panel corresponds to the gravity center of China's irrigated area for a specific year (ranging from 2000 to 2020). The spatial trend in irrigated area at the subregional scale has also been provided in Supplementary Figure S5. Please refer to our response to your second comment.

11. Please also discuss the potential use of CIrrMap250, who will be interested in using this data? Science communities, Hydrologic models? Climate models? Or water resource managers?

Response: Following your suggestion, we briefly discussed the potential use of CIrrMap250 in the revised manuscript. However, more specific uses are dependent on users and actual applications.

Despite these limitations, CIrrMap250 makes a valuable contribution to the field of irrigation mapping and is poised to significantly support agricultural, hydrological, and climate studies, as well as water resource management in China. Ongoing efforts to address these limitations and explore potential enhancements will undoubtedly improve the accuracy and utility of our irrigation maps in the future. One of the major applications of CIrrMap250 will be estimating irrigation water use or requirements, considering that irrigated area is a dominate driver of irrigation water withdrawal (Ozdogan and Gutman, 2008; Puy et al., 2021). Secondly, the spatial detail provided by CIrrMap250 can be integrated into crop, hydrological, and climate models to improve the simulations of water uses and land-atmosphere interactions (Uniyal and Dietrich, 2021; Mcdermid et al., 2023; Yang et al., 2023). This integration will advance our understanding of how irrigation practices influence crop yield, and hydrological and climatic processes from local to nationwide scales. Lastly, CIrrMap250 provides insights into irrigation changes and can assist in optimizing the spatial distribution of irrigated croplands (Rosa et al., 2020a; Rosa et al., 2020b), thereby supporting more informed decisions for sustainable water and land use.

Minor comments:

1: L17-20: "...reconciled them with remote sensing data … integrated with multiple remote sensing data …" These two sentences seem redundant.

Response: These sentences describe the data sources utilized in developing CIrrMap250, as well as the primary method employed for data integration. This information is crucial and has been retained.

We harmonized irrigation statistics and surveys and reconciled them with remote sensing data. The refined estimates of irrigated area were then integrated with multiple remote sensing data (i.e., vegetation indices, hybrid cropland product, and paddy field maps) and an irrigation suitability map through a semi-automatic training approach.

2: L94: "both cropland and other land use"

Response: Revised.

This leads to the widespread presence of mixed pixels where cropland and other land use/cover types coexist.

3: L231: "with the assumption that"

Response: Revised.

The peak vegetation index was subsequently adjusted by irrigation suitability (Eq. 5), with the assumption that irrigated cropland, being greener and more productive, is also more suitable for irrigation compared to rainfed cropland.

4: 3.3 L265-270 and 3.3.3 L310-323, these texts seem similar and redundant.

Response: Thanks for the suggestion. The content in "3.3 L265-270" has been removed.

References

Chen, F., Zhao, H., Roberts, D., Van de Voorde, T., Batelaan, O., Fan, T., and Xu, W.: Mapping center pivot irrigation systems in global arid regions using instance segmentation and analyzing their spatial relationship with freshwater resources, Remote Sensing of Environment, 297, 113760, 10.1016/j.rse.2023.113760, 2023.

Chen, J., Chen, J., Liao, A., Cao, X., Chen, L., Chen, X., He, C., Han, G., Peng, S., Lu, M., Zhang, W., Tong, X., and Mills, J.: Global land cover mapping at 30m resolution: A POK-based operational approach, ISPRS Journal of Photogrammetry and Remote Sensing, 103, 7-27, 10.1016/j.isprsjprs.2014.09.002, 2015.

Dong, J., Fu, Y., Wang, J., Tian, H., Fu, S., Niu, Z., Han, W., Zheng, Y., Huang, J., and Yuan, W.: Early-season mapping of winter wheat in China based on Landsat and Sentinel images, Earth System Science Data, 12, 3081-3095, 10.5194/essd-12-3081-2020, 2020.

Li, H. and Chen, Y.: Assessing potential land suitable for surface irrigation using groundwater data and multi-criteria evaluation in Xinjiang inland river basin, Computers and Electronics in Agriculture, 168, 105079, 10.1016/j.compag.2019.105079, 2020.

Liu, J., Kuang, W., Zhang, Z., Xu, X., Qin, Y., Ning, J., Zhou, W., Zhang, S., Li, R., Yan, C., Wu, S., Shi, X., Jiang, N., Yu, D., Pan, X., and Chi, W.: Spatiotemporal characteristics, patterns, and causes of land-use changes in China since the late 1980s, Journal of Geographical Sciences, 24, 195-210, 10.1007/s11442-014-1082-6, 2014.

Liu, Y., Li, Q., and Wu, W.: Analysis of feature slection for mapping irrigated cropland in northern China (In Chinese), Chinese Journal of Agricultural Resources and Regional Planning, 42, 27-35, 2022.

Mei, Q., Zhang, Z., Han, J., Song, J., Dong, J., Wu, H., Xu, J., and Tao, F.: ChinaSoyArea10m: a dataset of soybean planting areas with a spatial resolution of 10 m across China from 2017 to 2021, Earth Syst. Sci. Data Discuss., 2023, 1-27, 10.5194/essd-2023-467, 2023.

Meier, J., Zabel, F., and Mauser, W.: A global approach to estimate irrigated areas – a comparison between different data and statistics, Hydrology and Earth System Sciences, 22, 1119-1133, 10.5194/hess-22-1119-2018, 2018.

Potapov, P., Turubanova, S., Hansen, M. C., Tyukavina, A., Zalles, V., Khan, A., Song, X.-P., Pickens, A., Shen, Q., and Cortez, J.: Global maps of cropland extent and change show accelerated cropland expansion in the twenty-first century, Nature Food, 10.1038/s43016-021-00429-z, 2021.

Shahriar Pervez, M., Budde, M., and Rowland, J.: Mapping irrigated areas in Afghanistan over the past decade using MODIS NDVI, Remote Sensing of Environment, 149, 155-165, 10.1016/j.rse.2014.04.008, 2014.

Shen, R., Dong, J., Yuan, W., Han, W., Ye, T., and Zhao, W.: A 30 m Resolution Distribution Map of Maize for China Based on Landsat and Sentinel Images,

Journal of Remote Sensing, 2022, 10.34133/2022/9846712, 2022.
Shen, R., Pan, B., Peng, Q., Dong, J., Chen, X., Zhang, X., Ye, T., Huang, J., and Yuan, W.: High-resolution distribution maps of single-season rice in China from 2017 to 2022, Earth Syst. Sci. Data, 15, 3203-3222, 10.5194/essd-15-3203-2023, 2023.
Thenkabail, P. S., Biradar, C. M., Noojipady, P., Dheeravath, V., Li, Y., Velpuri, M., Gumma, M., Gangalakunta, O. R. P., Turral, H., Cai, X., Vithanage, J., Schull, M. A., and Dutta, R.: Global irrigated area map (GIAM), derived from remote sensing, for the end of the last millennium, International Journal of Remote Sensing, 30, 3679-3733, 10.1080/01431160802698919, 2009.
Tian, X., Dong, J., Chen, X., Zhou, J., Gao, M., Wei, L., Kang, X., Zhao, D., Zhang, H., Crow, W. T., Huang, R., Shao, W., and Zhou, H.: County-Level Evaluation of Large-Scale Gridded Data Sets of Irrigated Area Over China, Journal of Geophysical Research: Atmospheres, 129, e2023JD040333, https://doi.org/10.1029/2023JD040333, 2024.
Van Tricht, K., Degerickx, J., Gilliams, S., Zanaga, D., Battude, M., Grosu, A., Brombacher, J., Lesiv, M., Bayas, J. C. L., Karanam, S., Fritz, S., Becker-Reshef, I., Franch, B., Mollà-Bononad, B., Boogaard, H., Pratihast, A. K., and Szantoi, Z.: WorldCereal: a dynamic open-source system for global-scale, seasonal, and reproducible crop and irrigation mapping, Earth Syst. Sci. Data, 2023, 1-36, 10.5194/essd-2023-184, 2023.
Worqlul, A. W., Collick, A. S., Rossiter, D. G., Langan, S., and Steenhuis, T. S.: Assessment of surface water irrigation potential in the Ethiopian highlands: The Lake Tana Basin, Catena, 129, 76-85, 10.1016/j.catena.2015.02.020, 2015.
Worqlul, A. W., Jeong, J., Dile, Y. T., Osorio, J., Schmitter, P., Gerik, T., Srinivasan, R., and Clark, N.: Assessing potential land suitable for surface irrigation using groundwater in Ethiopia, Applied Geography, 85, 1-13, 10.1016/j.apgeog.2017.05.010, 2017.
Xie, Y., Lark, T. J., Brown, J. F., and Gibbs, H. K.: Mapping irrigated cropland extent across the conterminous United States at 30 m resolution using a semi-automatic training approach on Google Earth Engine, ISPRS Journal of Photogrammetry and Remote Sensing, 155, 136-149, 10.1016/j.isprsjprs.2019.07.005, 2019.
Yang, J. and Huang, X.: The 30 m annual land cover dataset and its dynamics in China from 1990 to 2019, Earth Syst. Sci. Data, 13, 3907-3925, 10.5194/essd-13-3907-2021, 2021.
You, N., Dong, J., Huang, J., Du, G., Zhang, G., He, Y., Yang, T., Di, Y., and Xiao, X.: The 10-m crop type maps in Northeast China during 2017–2019, Scientific Data, 8, 10.1038/s41597-021-00827-9, 2021.
Yu, Z., Jin, X., Miao, L., and Yang, X.: A historical reconstruction of cropland in China from 1900 to 2016, Earth System Science Data, 13, 3203-3218, 10.5194/essd-13-3203-2021, 2021.
Zhang, C., Dong, J., and Ge, Q.: IrriMap_CN: Annual irrigation maps across China in 2000–2019 based on satellite observations, environmental variables, and

machine learning, Remote Sensing of Environment, 280, 113184, 10.1016/j.rse.2022.113184, 2022a.

Zhang, H., Lou, Z., Peng, D., Zhang, B., Luo, W., Huang, J., Zhang, X., Yu, L., Wang, F., Huang, L., Liu, G., Gao, S., Hu, J., Yang, S., and Cheng, E.: Mapping annual 10-m soybean cropland with spatiotemporal sample migration, Scientific Data, 11, 439, 10.1038/s41597-024-03273-5, 2024a.

Zhang, L., Wang, W., Ma, Q., Hu, Y., and Zhao, Y.: CCropLand30: High-resolution hybrid cropland maps of China created through the synergy of state-of-the-art remote sensing products and the latest national land survey, Computers and Electronics in Agriculture, 218, 108672, 10.1016/j.compag.2024.108672, 2024b.

Zhang, L., Zhang, K., Zhu, X., Chen, H., and Wang, W.: Integrating remote sensing, irrigation suitability and statistical data for irrigated cropland mapping over mainland China, Journal of Hydrology, 613, 128413, 10.1016/j.jhydrol.2022.128413, 2022b.